Fully Automatic Quantitative Software for Assessment of Minute Finger Joint Space Narrowing Progression on Radiographs: Evaluation in Rheumatoid Arthritis Patients with long-term sustained clinical low disease activity

Abstract

Purpose: Rheumatoid arthritis (RA) causes joint space narrowing (JSN) as a form of joint destruction. We developed an automatic system that can detect joint locations and compute the joint space difference index (JSDI), which was defined as the chronological change in JSN between two radiographs. This study aims to evaluate the application of "machine vision" for radiographic image of the finger joints.

Materials and methods: Fifteen RA patients with long-term sustained clinical low disease activity were recruited. All patients underwent hand radiography and power Doppler ultrasonography (PDUS). The JSN was evaluated using the Genant-modified Sharp scoring (GSS) method and the automatic system. Synovial vascularity (SV) was assessed quantitatively using ultrasonography.

Results: There were no significant differences in the JSDI between the joints with JSN and those without JSN on GSS ($p = 0.052$). The JSDI of the joints with SV was significantly higher than those without SV ($p = 0.043$). The JSDI of the no therapeutic response group was significantly higher than those of the response group ($p < 0.001$).

Conclusion: Our software can automatically evaluate temporal changes of JSN, which might free rheumatologists / radiologists from the burden of scoring hand radiography.

Secondary Abstract

We developed an automatic system that can detect joint locations and compute the joint space difference

index (JSDI), which was defined as the chronological change in JSN between two radiographs. Our software can automatically measure temporal changes of JSN.

Keywords: Rheumatoid arthritis; Radiography; Ultrasonography; Synovial vascularity; joint space narrowing

Introduction

Rheumatoid arthritis (RA) is one of the most common, chronic autoimmune diseases. Articular cartilage and bone are damaged by synovitis, resulting in joint space narrowing (JSN) and bone erosion (1-3). This is irreversible damage which progresses rapidly within a year of onset (4-6). Treatment of RA during the "window of opportunity," in which disease activity is lower with limited inflammatory cell infiltration and response to treatment is higher, is more likely to retard disease progression (7). Since around the turn of the 21st century, introduction of new therapeutics, including biological agents, have made it possible to achieve a significant level of low disease activity or remission within a certain period of time (8). Therefore, minute joint damage changes need to be detected in order to assess therapeutic effects (9).

Currently, radiography is the main tool for the diagnosis and monitoring of RA because of its wide availability, relatively low cost and high capability for imaging bones and joints. The Sharp/van der Heijde scoring method and the Genant-modified Sharp scoring (GSS) method, both of which score radiographic progression in RA, have been used as the gold standard in many clinical studies (10, 11). However, there are limitations in sensitivity and reproducibility, because these semi-quantitative methods are based on visual assessments by radiologists (12).

The automatic measurement of joint space width, which is able to identify joint space difference on the order of 1 mm or less and also reduces the time and energy required for analysis, has recently received much attention. Some studies have shown that joint margin delineation with a high success rate and joint space measurement produced highly sensitive and reproducible results. However, a false margin may be

projected over or under the true margin, due to the concave structure of the distal margin for the metacarpophalangeal (MCP) joint, sometimes causing failure of margin delineation (13-16). Moreover, most studies excluded the first joints from joint space analysis because of difficult margin delineation, caused by structural differences from other fingers and the oblique projection of the thumb (14, 15, 17).

In a study by Ichikawa et al. (18), software assessed the JSN without margin detection using the joint space narrowing index (JSDI), which was defined as the difference of pixel values between two radiographs applying a temporal subtraction technique. Although the software using JSDI demonstrated high accuracy beyond human eyes, even by a non-expert of imaging analysis, manual operations were needed such as image registration of the baseline and follow-up radiographs, and region of interest (ROI) placement (19-22).

In this paper, we developed an automatic system that can detect joint location of the finger joints, place ROIs in the joints, perform image registration, and compute the JSDI, which was compared with GSS. This application of "machine vision" for radiographic image was further validated using quantitative power Doppler sonography for synovial vascularity which precede the progression of local finger joint damage (23).

Materials and Methods

Patients

Fifteen patients (2 men, 13 women) who fulfilled the 1987 American Rheumatism Association classification criteria for RA were recruited for this study. All patients had sustained long-term clinical low disease activity (disease activity score with 28 joints–erythrocyte sedimentation rate [DAS28-ESR] < 3.2). The median duration of disease and clinical low disease activity were 50 months (range 26-196) and 15 months (range 12-19), respectively. The treatments were carried out with non-biologic disease-modifying antirheumatic drugs (DMARDs) (methotrexate [MTX], n = 8; MTX + tacrolimus, n = 3) or with biological DMARDs (MTX + adalimumab, n = 1; MTX + tocilizumab [TCZ], n = 2; TCZ monotherapy, n = 1). The subjects have been described previously (24). Clinical and laboratory characteristics of the patients at the baseline are shown in Table 1. The study was conducted in compliance with the Declaration of Helsinki and approved by the local ethics committee. Informed consent was obtained in the form of opt-out on the website.

Radiography

Hand radiographs were obtained from patients at the baseline and at the 52nd week. All radiographs were taken in a posterior-anterior view by digital X-ray equipment (Radnext 32; Hitachi, Tokyo, Japan) under the following standard conditions: X-ray aluminum filter thickness = 0.5 mm; tube voltage = 50 kV; tube current = 100 mA; exposure time = 25 msec; film focus distance = 100 cm. The center of the X-ray beam was the MCP joint of the second finger. Radiographs were displayed as digital imaging and communications

in medicine (DICOM) images with 2010 by 1670 pixels, and a 0.15× 0.15 mm pixel size at 10-bit grayscale resolution.

The radiological progression of the finger joints from baseline to the 52nd week was examined according to the local JSN assessment of the GSS by a rheumatologist with more than 20 years of experience, who was blinded to other clinical information.

Ultrasonography

Ultrasonography (US) was performed at the baseline and 8th, 20th and 52nd weeks by one of three US experts who specialized in musculoskeletal US, with experience in joint ultrasound for 12-18 years, who were blinded to other clinical information. The first through fifth MCP and second through fifth proximal interphalangeal (PIP) joints were scanned over the dorsal surface in the transverse with light skin pressure by a 13 MHz linear array transducer (Avius; Hitachi Aloka Medical, Ltd., Tokyo, Japan). The power Doppler setting was as follows: 1.3 kHz pulse repetition frequency, 75 dB dynamic range, medium persistence, medium frame rate, low wall filter, flow optimization: medium vain, and 1.3 kHz speed velocity.

The power Doppler ultrasonography images were used for quantitative assessment of synovial vascularity (SV). SV value was determined by counting the number of vascular flow pixels in the region of interest (ROI). A rectangular ROI with a size of 5 mm × 10 mm was located, in order to contain as many of the vascular flow pixels as possible.

In-house software

An application was developed in-house to automatically locate each joint and compute the JSDI. The software uses the pattern matching module of Matrox Imaging Library (MIL) version 9.0, running on 64-bit Windows 7. Pattern matching is a method for locating a small model image within a larger target image. The MIL package computes the normalized grayscale correlation (NGC) between the model image and the target image at various candidate locations. Rotations can be optionally enabled. A pattern recognition score is computed from the NGC for several locations within the target and the location with the highest score is retuned by MIL. The pattern recognition score has a value from 0 to 100, with 100 indicating a perfect match. Efficiently computing the optimal position of the model within the target with the maximum pattern recognition score from a minimum number of candidate positions is a difficult programming challenge. That is why we chose to use a commercial library. The disadvantage is that a run-time license must be purchased from Matrox for each installation of the software.

Before the software can be used, models for each joint must be created for the left and right hand. This is a one-time setup process; the models can be used with all subsequent diagnostic images. A model consists of a bitmap of a hand and three ROIs specifying the hand, bone and joint regions (Figure 1). To create a new model, first open a typical baseline image. The typical image should be relatively disease-free so that the target joint is not severely damaged. A hand ROI is placed to specify the approximate left or

right hand region. The size of the hand ROI should be large enough to include most of the finger bones. In our tests, the hand ROI size was 800 by 600 pixels. The hand ROI is used as a pattern match model to locate the general location of the left or right hand.

A second ROI specifies the bones containing the target joint. The bone ROI helps to prevent mistakes between adjacent fingers (to the left or right) and between MCP and PIP joints above or below. The bone ROI is used as a pattern search model within the region of the hand.

The user then specifies a third ROI, specifying the joint of interest. The size of the joint ROI was 80 by 20 pixels in our tests. The joint ROI can be rotated to match the angle of the joint. The joint ROI is searched for within the region of the bone ROI.

The bitmap of the hand ROI is saved in a TIFF file, along with the offset and size of the hand, bone and joint ROIs. A single model is saved for each joint for the left and right hand. To account for variations of anatomy (for example male and female), multiple models can be defined for each joint.

To compute the JSDI, the user first opens the baseline and follow-up hand radiographs. The user then specifies one or more joint models from a list of defined joints (MCP1-5, PIP1-5) for the left or right hand. Alternatively, the software can be operated in batch mode where all joints are processed sequentially, saving the results in a CSV file. The software first automatically determines the approximate location of the base image hand region using the hand model bitmap read from the TIFF file. If multiple models for a single joint were specified, the bitmap with the highest pattern matching score is used. The baseline target

image is rotated to match the hand model image as closely as possible.

Next, the position of the hand ROI is used to initially place the bone ROI within the hand ROI on the baseline image. The bitmap of the bone ROI model is then used for a secondary search within the hand ROI region. In this step, rotation is disabled because the axial alignment of the wrist was already determined in the previous step. Finally, the joint ROI is searched within the region of the bone ROI. Rotation is enabled to find the best possible match.

Once the position of the desired joint has been located on the baseline image, the follow-up image is searched with the same three-step process used for the baseline image. A bitmap taken from the hand ROI on the baseline image is used as a model to search within the follow-up image. The follow-up image is rotated in order to maximize the pattern recognition score. A bitmap taken from the bone ROI on the baseline image is then searched within the hand ROI, again without rotation. Finally, the joint ROI from the baseline image is searched within the bone ROI on the follow-up image.

The joint region of the baseline and follow-up images should now be aligned as closely as possible, maximizing the pattern recognition score. The user can now direct the software to compute the JSDI, which considers each pixel within the joint ROI.

The width of the rectangular joint ROI was shrunk by 80, 60, 40, and 20 percent from the joint center, in order to investigate the optimum ROI size to efficiently detect JSN. The software requires approximately one second to process a single joint (i.e. detecting joint location, placing ROI in the joints,

performing image registration, and computing the JSDI in all for one finger joint) on the standard PC that we tested on. For our tests, the software was operated by a non-specialist (BLINDED). Given the same input radiograph and joint models, the software will reproduce the same JSDI perfectly (100%).

Statistical analysis

Statistical analyses were performed using IBM SPSS version 24.0 (IBM) for Windows (Microsoft). All tests were bilateral and the level for significance set to $p < 0.05$. We defined ΔGSS as score change in GSS between at the baseline and at the 52nd week. We compared the JSDI between joints with JSN progression (the ΔGSS [+] group) and without JSN progression (the ΔGSS [-] group) in score change interval at the baseline and at the 52nd week on GSS. We next focused on the ΔGSS (-) group in order to confirm that the JSDI can detect minute changes which were led by SV and not scored by observers. We divided the ΔGSS (-) group into two groups: joints without SV at the baseline and during the follow-up period (the SV [-] group), and those with SV at least once at the baseline and during the follow-up period (the SV [+] group). We also categorized those finger joints into two groups: the therapeutic response (R) group, in which the presence of SV was not observed during the observation period and the presence of SV was observed limited to the period from the baseline to week 8; and the no therapeutic response (NR) group, which contained all the other joints. The JSDI between the SV (-) and SV (+) groups, and between the R and NR groups were evaluated using the Mann-Whitney U test.

Intra-observer agreement of visual assessment was estimated by calculating the intra-class correlation coefficients (ICC), employing a one-way random effect model for intra-observer agreement.

Results

In total, 256 finger joints were analyzed. Severely damage joints including complete luxation, subluxation, and improved score according to the GSS ($\Delta GSS < 0$), were excluded before analysis. Figure 2 shows examples of excluded joints. The success rates of automatic measurement were 98.6% (138/140) and 97.4% (113/116) for MCP and PIP joints, respectively. For the MCP joints of the thumb, 100% were measured automatically. The ROI locations of 5 joints in 3 patients were determined to be incorrect by a rheumatologist. An example of a false case in the joint location detection is shown in Figure 3.

Out of 251 joints, 35 joints were assigned to the ΔGSS (+) group, and the rest were assigned to the ΔGSS (-) group. There were no significant differences in the JSDI between the ΔGSS (+) and ΔGSS (-) groups in all sizes of ROI (Table 2).

Out of the ΔGSS (-) group, the number of joints in the SV (+) and SV (-) group were 28 and 188, respectively. The JSDI of the SV (+) group was significantly higher than the JSDI of the SV (-) group in all sizes of ROI (Table 3).

Eighteen joints were categorized as the NR group and 198 joints were categorized as the R group from the ΔGSS (-) group. The JSDI of the NR group was significantly higher than the JSDI of the R group

in all sizes of ROI (Table 4).

Intra-observer reliability for the baseline GSS and follow-up GSS was in substantial agreement (ICC = 0.730; 95% CI = 0.668–0.782 and ICC = 0.718; 95% CI = 0.653–0.772, respectively). Intra-observer reliability for ΔGSS was in moderate agreement (ICC = 0.490; 95% CI = 0.392–0.577).

Discussion

We evaluated our in-house software for assessing JSN progression of the finger joints on radiographs between baseline and follow-up images. We found that our software marginally failed to differentiate between JSN progression and JSN non-progression joints determined by human assessment. On the contrary, it could identify the difference in JSN progression, which was not recognized by human assessment, according to synovitis as a risk for JSN progression evaluated with power Doppler ultrasonography. This discrepancy might be explained by different mechanism in image recognition between software and human. Our software might be effectively utilized in clinical trials, where considerable time and efforts of rheumatologists/radiologists are required for image scoring.

The automatic measurement of joint space width has recently been shown to be useful in several studies (13-17). These studies measured and validated joint space width transversely rather than longitudinally. Huo et al.(25) compared as proof of concept of the sensitivity to change of automated quantification of radiographic wrist and hand joint space width of 1-2 years by scoring JSW according to

the Sharp/van der Heijde scoring method in two strategy groups of a treat-to-target and tight-control early RA study. To our knowledge, the present study is the first study to prove the usefulness of software that automatically evaluates temporal changes of JSN in established RA patients, although highly deformed joints were excluded from the analysis. The primary difference between our method and earlier methods is that we do not attempt to measure the joint space width directly; instead we compute the change in pixel values in the registered baseline and follow-up images. Furthermore, we utilize a commercial pattern matching library (MIL) to automatically locate the joints.

The proposed method showed a high success rate for joint location detection on analyzed joints at 98.6% (138/140) and 97.4% (113/116) for MCP and PIP joints, respectively. For the MCP joints of the thumb, 100% were measured automatically. The software works by detecting the difference in the pixel values of the ROI at the finger joint between the baseline and follow-up images due to JSN progression after modification of the ROI size. In particular, the success rate was 100% for the MCP joint on the thumb, which was considered to have structural differences with other fingers, making it difficult to delineate the margin by oblique projection. The success rate was higher than that of location detection for the MCP joint on the thumb in previous studies (Zielinski et al. reported 93.7% (26), and Huo et al. reported 94.7% (13)). We considered that few cases deviated from the created model and that identification of the joint of interest in stages led to high location detectability, where the ROI could not be set correctly due to the effects of JSN and bone erosion near the joint.

The SV in each joint space was quantitatively measured using a power Doppler ultrasound image. Fukae et al. (24) have previously demonstrated that this quantitative method can assess SV, and reported that finger joints with positive SV resulted in joint destruction determined by the visual assessment of the GSS method even if clinical low disease activity was sustained over 1 year. Therefore, we considered that minute JSN progression can be predicted by the presence of SV. In order to show the superiority of the software over visual assessment, the joints without score change between the baseline and follow-up on GSS ware targeted. We confirmed that there was a difference in JSN depending on the presence of SV. This result corresponded to the results of a previous study (24). Moreover, the difference was remarkable when the grouping was based on observation of SV at the 8th week from the baseline. The joints in which SV disappeared by the 8th week due to the treatment may not be caused by the progression of minute JSN. In this study, the software was able to automatically detect fine joint space narrowing that could not be detected by visual assessment.

Some limitations of this study should be mentioned. First, the number of patients was relatively small. Study with more cases is warranted. Second, the ROI could not be set correctly when the joints were severely damaged with ankylosis, complete luxation or subluxation. We need to develop a system for the automatic recognition and exclusion of severely damaged joints that can lead to exact ROI placement in all joints. Third, the JSDI may be affected by inadequate hand positioning. In order to ensure accuracy and reliability in measurements, it is necessary to perform standardized hand positioning. In this study, the hand

positioning was performed according to the procedure carefully standardized before images were obtained. Finally, we need to improve the software to make it easier to use, especially the process of defining joint models.

In conclusion, we developed an automatic system that can detect joint location, place a ROI around the joint, perform image registration, and compute the JSDI in order to evaluated JSN progression in RA patients. The software therefore has potential to be useful for evaluation of therapeutic outcome in patients of RA during the early stage of the disease.

References

1. Bartok B, Firestein GS. Fibroblast-like synoviocytes: key effector cells in rheumatoid arthritis. Immunol Rev. 2010;233(1):233-55.

2. Bottini N, Firestein GS. Duality of fibroblast-like synoviocytes in RA: passive responders and imprinted aggressors. Nat Rev Rheumatol. 2013;9(1):24-33.

3. Karsdal MA, Woodworth T, Henriksen K, Maksymowych WP, Genant H, Vergnaud P, et al. Biochemical markers of ongoing joint damage in rheumatoid arthritis--current and future applications, limitations and opportunities. Arthritis Res Ther. 2011;13(2):215.

4. van der Heijde DM, van Leeuwen MA, van Riel PL, van de Putte LB. Radiographic progression on radiographs of hands and feet during the first 3 years of rheumatoid arthritis measured according to Sharp's method (van der Heijde modification). J Rheumatol. 1995;22(9):1792-6.

5. Plant MJ, Jones PW, Saklatvala J, Ollier WE, Dawes PT. Patterns of radiological progression in early rheumatoid arthritis: results of an 8 year prospective study. J Rheumatol. 1998;25(3):417-26.

6. Machold KP, Stamm TA, Eberl GJ, Nell VK, Dunky A, Uffmann M, et al. Very recent onset arthritis--clinical, laboratory, and radiological findings during the first year of disease. J Rheumatol. 2002;29(11):2278-87.

7. Boers M. Understanding the window of opportunity concept in early rheumatoid arthritis. Arthritis Rheum. 2003;48(7):1771-4.

8. Kaneko Y, Takeuchi T. A paradigm shift in rheumatoid arthritis over the past decade. Intern Med. 2014;53(17):1895-903.

9. Bakker MF, Jacobs JW, Verstappen SM, Bijlsma JW. Tight control in the treatment of rheumatoid arthritis: efficacy and feasibility. Ann Rheum Dis. 2007;66 Suppl 3:iii56-60.

10. van der Heijde DM. Plain X-rays in rheumatoid arthritis: overview of scoring methods, their reliability and applicability. Baillieres Clin Rheumatol. 1996;10(3):435-53.

11. Genant HK, Jiang Y, Peterfy C, Lu Y, Redei J, Countryman PJ. Assessment of rheumatoid arthritis using a modified scoring method on digitized and original radiographs. Arthritis Rheum. 1998;41(9):1583-90.

12. Sharp JT, Wolfe F, Lassere M, Boers M, Van Der Heijde D, Larsen A, et al. Variability of precision in scoring radiographic abnormalities in rheumatoid arthritis by experienced readers. J Rheumatol. 2004;31(6):1062-72.

13. Huo Y, Vincken KL, van der Heijde D, De Hair MJ, Lafeber FP, Viergever MA. Automatic Quantification of Radiographic Finger Joint Space Width of Patients With Early Rheumatoid Arthritis. IEEE Trans Biomed Eng. 2016;63(10):2177-86.

14. van 't Klooster R, Hendriks EA, Watt I, Kloppenburg M, Reiber JH, Stoel BC. Automatic quantification of osteoarthritis in hand radiographs: validation of a new method to measure joint space width. Osteoarthritis Cartilage. 2008;16(1):18-25.

15. Langs G, Peloschek P, Bischof H, Kainberger F. Automatic quantification of joint space narrowing and erosions in rheumatoid arthritis. IEEE Trans Med Imaging. 2009;28(1):151-64.

16. Bielecki A, Korkosz M, Zieliński B. Hand radiographs preprocessing, image representation in the finger regions and joint space width measurements for image interpretation. Pattern Recognition. 2008;41(12):3786-98.

17. Duryea J, Jiang Y, Zakharevich M, Genant HK. Neural network based algorithm to quantify joint space width in joints of the hand for arthritis assessment. Med Phys. 2000;27(5):1185-94.

18. Ichikawa S, Kamishima T, Sutherland K, Okubo T, Katayama K. Performance of computer-based analysis using temporal subtraction to assess joint space narrowing progression in rheumatoid patients. Rheumatol Int. 2016;36(1):101-8.

19. Ichikawa S, Kamishima T, Sutherland K, Okubo T, Katayama K. Radiographic quantifications of joint space narrowing progression by computer-based approach using temporal subtraction in rheumatoid wrist. Br J Radiol. 2016;89(1057):20150403.

20. Hatano K, Kamishima T, Sutherland K, Kato M, Nakagawa I, Ichikawa S, et al. A reliability study using computer-based analysis of finger joint space narrowing in rheumatoid arthritis patients. Rheumatol Int. 2017;37(2):189-95.

21. Okino T, Kamishima T, Lee Sutherland K, Fukae J, Narita A, Ichikawa S, et al. Radiographic temporal subtraction analysis can detect finger joint space narrowing progression in rheumatoid arthritis with clinical low disease activity. Acta Radiol. 2018;59(4):460-7.

22. Kato K, Yasojima N, Tamura K, Ichikawa S, Sutherland K, Kato M, et al. Detection of Fine Radiographic Progression in Finger Joint Space Narrowing Beyond Human Eyes: Phantom Experiment and Clinical Study with Rheumatoid Arthritis Patients. Sci Rep. 2019;9(1):8526.

23. Fukae J, Kon Y, Henmi M, Sakamoto F, Narita A, Shimizu M, et al. Change of synovial vascularity in a single finger joint assessed by power doppler sonography correlated with radiographic change in rheumatoid arthritis: comparative study of a novel quantitative score with a semiquantitative score. Arthritis Care Res (Hoboken). 2010;62(5):657-63.

24. Fukae J, Isobe M, Kitano A, Henmi M, Sakamoto F, Narita A, et al. Structural deterioration of finger joints with ultrasonographic synovitis in rheumatoid arthritis patients with clinical low disease activity. Rheumatology (Oxford). 2014;53(9):1608-12.

25. Huo Y, Veldhuizen RD, van der Heijde DM, Besselink NJ, Jacobs JW, van Laar JM, et al. Automated joint space width quantification of hand and wrist joints: a proof of concept study. Clin Exp Rheumatol. 2016;34(5 Suppl 101):S34-S9.

26. Zeliński B. Hand radiograph analysis and joint space location improvement for image interpretation Schedae Informat. 2009;17(1):45-61.

Table

Table 1. Clinical characteristics of RA patients at baseline

Characteristic	
Total no. of patients included	15
Age, median (range) years	54 (32 - 69)
Sex, female/male	13/2
Duration of disease, median (range) months	50 (26 - 196)
Duration of CLDA, median (range) months	15 (12 - 19)
Swollen joint count, range	0 - 2
Tender joint count, range	0 - 2
DAS28-ESR, mean (SD)	2.03 (0.55)

CLDA, clinical low disease activity; DAS28, disease activity score with 28 joints; ESR, erythrocyte sedimentation rate; SD, standard deviation

Table 2. JSDI values in ΔGSS(-) and ΔGSS(+) groups in each ROI size

ROI size	20%	40%	60%	80%	100%
ΔGSS(-)	58.0 (22.1-224)	58.0 (23.9-225)	57.5 (24.7-222)	57.5 (23.6-217)	56.7 (24.0-210)
ΔGSS(+)	68.1 (28.2-182)	71.1 (26,6-182)	70.4 (28.4-183)	68.6 (29.9-178)	65.4 (31.7-169)
p value[a]	0.13	0.10	0.077	0.094	0.052

Values are given in median (range)

ΔGSS, delta Genant-modified Sharp score; ROI, region of interest

[a]Mann-Whitney U test

Table 3. JSDI values in SV(-) and SV(+) groups in each ROI size

ROI size	20%	40%	60%	80%	100%
SV(-)	57.1 (22.1-224)	57.0 (23.9-225)	55.6 (24.7-222)	55.2 (23.6-217)	55.5 (24.0-210)
SV(+)	68.2 (25.5-199)	72.6 (28.2-201)	72.0 (31.7-201)	70.0 (32.7-199)	67.1 (30.6-194)
p value[a]	0.023*	0.027*	0.028*	0.034*	0.043*

Values are given in median (range)

SV, synovial vascularity; ROI, region of interest

[a]Mann-Whitney U test

*Difference was significant ($p<0.05$)

Table 4. JSDI values in R and NR groups

ROI size	20%	40%	60%	80%	100%
R group	56.8 (22.1-224)	55.6 (23.9-225)	55.3 (24.7-222)	55.0 (23.6-217)	55.3 (24.0-210)
NR group	80.7 (25.5-199)	82.5 (28.2-201)	81.3 (34.5-201)	78.6 (33.8-199)	74.9 (35.5-194)
p value[a]	0.0011*	< 0.001*	< 0.001*	< 0.001*	< 0.001*

R, response; NR, no response

[a]Mann-Whitney U test

*Difference was significant ($p < 0.05$)

Figure legends

Fig. 1 Model created with a typical hand radiograph with hand, bone and finger joint ROI specification.

ROI, region of interest

Fig. 2 Sample excluded joints: (a) A joint with subluxation; (b) A joint with complete luxation.

Fig. 3 Sample joints with incorrect joint ROI. (a) highly narrowed joint space; (b) sclerosis of the bone; (c) presence of bone erosion at the lateral side of proximal middle phalanx.

ROI, region of interest

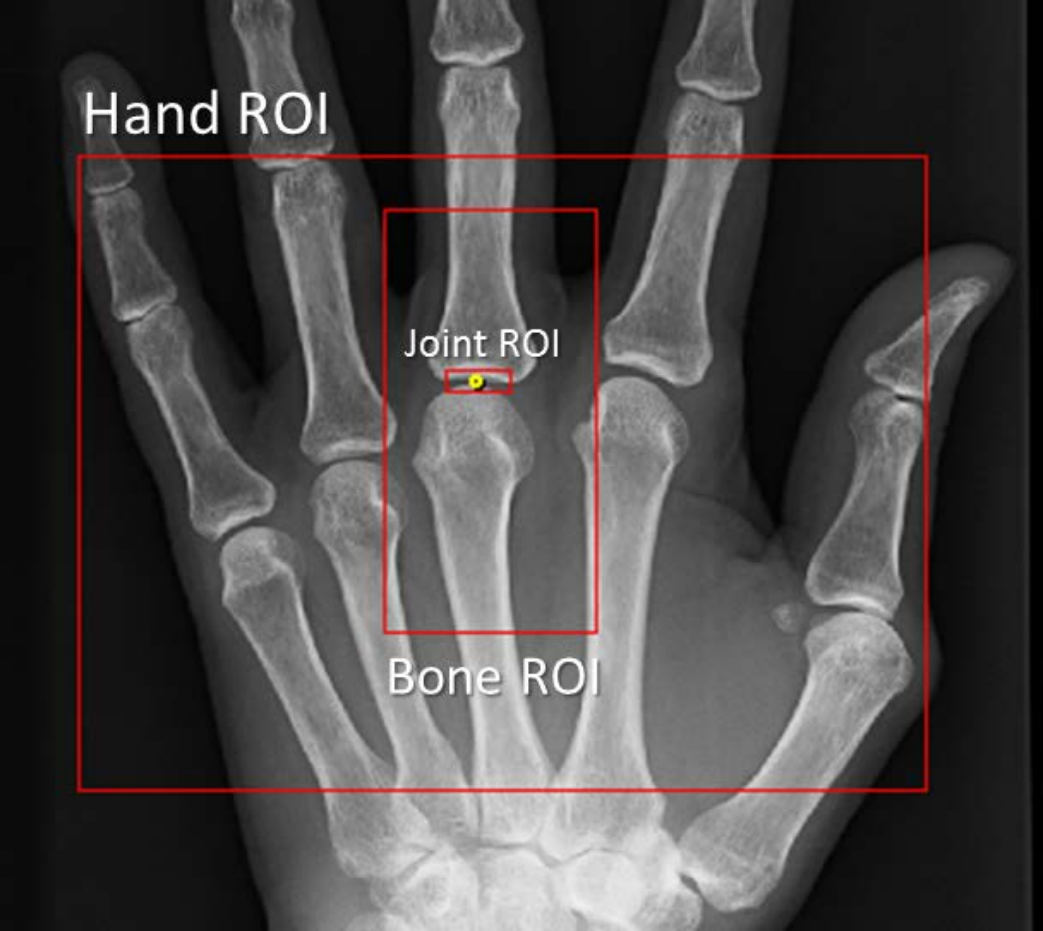
Hand ROI
Joint ROI
Bone ROI